

# Mixed $H_2/H_\infty$ Design for a Decentralized Discrete Variable Structure Control With Application to Mobile Robots

Chih-Lyang Hwang, *Associate Member, IEEE*, and Song-Yu Han

**Abstract**—In this paper, a decentralized discrete variable structure control via mixed  $H_2/H_\infty$  design was developed. In the beginning, the  $H_2$ -norm of output error and weighted control input was minimized to obtain a control such that smaller energy consumption with bounded tracking error was assured. In addition, a suitable selection of this weighted function (connected with frequency) could reduce the effect of disturbance on the control input. However, an output disturbance caused by the interactions among subsystems, modeling error, and external load deteriorated system performance or even brought about instability. In this situation, the  $H_\infty$ -norm of weighted sensitivity between output disturbance and output error was minimized to attenuate the effect of output disturbance. Moreover, an appropriate selection of this weighted function (related to frequency) could reject the corresponding output disturbance. No solution of Diophantine equation was required; the computational advantage was especially dominated for low-order system. For further improving system performance, a switching control for every subsystem was designed. The proposed control (mixed  $H_2/H_\infty$  DDVSC) was a three-step design method. The stability of the overall system was verified by Lyapunov stability criterion. The simulations and experiments of mobile robot were carried out to evaluate the usefulness of the proposed method.

**Index Terms**—Decentralized control,  $H_2$ -optimization,  $H_\infty$ -optimization, mobile robot, variable structure control.

## I. INTRODUCTION

IN THE PAST three decades, the properties of the interconnected systems have been widely studied [1]–[5]. Owing to the physical configuration and high dimensionality of interconnected systems, centralized control is neither economically feasible nor even necessary [2]. Because the decentralized control scheme is free from the difficulties arising from the complexity in design, debugging, data gathering, and storage requirements, it is more preferable for the interconnected systems than a centralized control (e.g., the decentralized control for a mobile robot [6] or a legged robot [7]). However, due to the existence of interactions among subsystems, modeling error, and external load, there are not many efficient decentralized controls for the interconnected systems. For simplifying the controller design, a linear discrete-time dynamic model for every

subsystem is first obtained by the recursive least squares parameter estimation. This kind of modeling is easier for the industry applications. However, every subsystem is assumed to be a linear dynamic system will be a challenge to obtain a decentralized control for the interconnected system.

Mixed  $H_2/H_\infty$  control problem has become a popular research topic in recent years (e.g., [8] and [9]). In engineering practice, the control input is designed not only to eliminate the disturbance but also to minimize a desired control performance when the worst disturbance is imposed. In this situation,  $H_2$ -optimization is more appealing for control engineering (e.g., [10]). In the other way,  $H_\infty$ -optimization is an important robust control methodology for diminishing effectively the effect of disturbance (e.g., [11]). Under this circumstance, the mixed  $H_2/H_\infty$  control problem is developed. It is also known that variable structure control contains several advantages, e.g., fast response, less sensitive to uncertainty, and easy implementation [12]–[15]. In this paper, the mixed  $H_2/H_\infty$  optimization and variable structure control are merged to improve the robust stability and robust performance.

In the beginning, the  $H_2$ -norm of the output error and weighted control input is minimized to obtain a control such that small energy consumption with bounded tracking error for every subsystem is achieved. In addition, a suitable selection of this weighted function can attenuate the effect of disturbance in a specific frequency range of control input. An appropriate application is the control problem of mobile robot with the battery power (e.g., [6]). However, an output disturbance brought about the interactions among subsystems, modeling error, and external load deteriorates system performance or even results in instability. In general, a mobile robot is controlled by a decentralized control to simplify the implementation of a digital control. However, the interactions of front and rear wheel, uneven road condition, often bring about a poor performance or even instability. In this situation, the  $H_\infty$ -norm of weighted sensitivity between output disturbance and output error of the  $i$ th subsystem is accomplished to attenuate the effect of output disturbance. Moreover, a suitable selection of weighted function can reject or attenuate the output disturbance in the desired frequency range. No solution of Diophantine equation is required; the computational advantage is especially dominated for low-order system. It indicates that a microprocessor-based control is realizable for the proposed control. Although the effect of output disturbance in a specific frequency range of the  $i$ th subsystem is attenuated or rejected, a better performance

Manuscript received March 23, 2004; revised August 25, 2004. This work was supported by the National Science Council of Taiwan, R.O.C. under Grant SC93-2218-E-036-003. This paper was recommended by Editor S. Phoha.

The authors are with the Department of Mechanical Engineering, Tatung University, Taipei, 10451 Taiwan, R.O.C. (e-mail: clhwang@ttu.edu.tw).  
Digital Object Identifier 10.1109/TSMCB.2005.845999

can be enhanced by a switching control based on the Lyapunov redesign [16]. Finally, the stability of the overall system is verified by Lyapunov stability criterion. The simulations and experiments of a mobile robot are also arranged to evaluate the effectiveness of the proposed controller.

## II. PROBLEM FORMULATION

Before describing the control problem, a mathematical notation of this paper is introduced as follows. A discrete-time signal at a  $k$  sampling interval (i.e.,  $kT_s$ ) of a continuous signal  $y(t)$  is represented by  $y(k) = y(kT_s) \in \mathfrak{R}$  where  $T_s$  denotes the sampling interval. A polynomial representation is defined as follows:  $A(z^{-1}) = a_0 + a_1z^{-1} + \dots + a_{n_a}z^{-n_a}$ , where  $a_i$  for  $i = 0, 1, \dots, n_a$  denote bounded coefficients,  $n_a$  stands for the system degree (i.e., if  $a_{n_a} \neq 0$ ,  $\deg\{A(z^{-1})\} = n_a$ ), and  $z^{-1}$  denotes the backward-time shift operator [i.e.,  $z^{-1}y(k) \equiv y(k-1)$ ] or a complex variable in the  $z$ -transform. Hence, the  $z$ -transform of a discrete-time signal  $y(k)$  is denoted by  $Y(z^{-1}) = Z\{y(k)\}$ . If  $a_0 = 1$  and it is called monic polynomial. The notations of  $A_+(z^{-1})$  and  $A_-(z^{-1})$  denote the stable and unstable part of  $A(z^{-1})$ , respectively. Without the loss of generality, the polynomial  $A_+(z^{-1})$  is assumed to be monic (i.e.,  $A_+(0) = 1$ ) to obtain a unique factorization. Define  $\|A(z^{-1})\|_2 = [\int_0^{2\pi} |A(e^{-j\theta})|^2 d\theta / 2\pi]^{1/2}$  where  $A \in H_2$ , the set  $H_2$  consists of all analytic functions  $A$  in  $|z| > 1$ . A rational function  $A(z^{-1})$  in  $H_2$  is inner if  $|A(e^{-j\theta})| = 1$  for all  $\theta \in [0, 2\pi]$ , and is outer if has no zeros in  $|z| > 1$ . For any rational functions  $Y(z^{-1})$  and  $Z(z^{-1})$  in  $H_2$  if  $Y(z^{-1})$  is inner function and  $\|Y(z^{-1})Z(z^{-1})\|_2$  is well defined, then  $\|Y(z^{-1})Z(z^{-1})\|_2 = \|Z(z^{-1})\|_2$ . A rational function multiplied by an inner function preserves the value of the norm [17]. The polynomial  $\bar{A}_-(z^{-1}) = z^{-n_a}A_-(z)$  is a stable polynomial. Then the rational function  $A_-(z^{-1})/\bar{A}_-(z^{-1})$  is a stable, causal, and all-pass operator, i.e.,  $|A_-(e^{-j\theta})/\bar{A}_-(e^{-j\theta})| = 1$  for  $0 \leq \theta \leq 2\pi$ . The notation  $\|A(z^{-1})\|_\infty = \text{ess. sup}_{0 \leq \theta \leq 2\pi} |A(e^{-j\theta})|$  is defined. The symbol  $A(z^{-1}, k)$  denotes a polynomial with time-varying coefficients which are bounded for all time. The upper script  $i$  denotes the  $i$ th subsystem of an interconnected system.

It is assumed that a linear dynamic interconnected system is expressed as follows:

$$y_p^i(k) = \frac{\{z^{-d^i} B_r^i(z^{-1}, k) u^i(k) + \sum_{j=1, j \neq i}^n z^{-d_j^i} B_j^i(z^{-1}, k) u^j(k)\}}{A_r^i(z^{-1}, k)} + \Delta^i(U(k), k), \quad i = 1, 2, \dots, n \quad (1)$$

where  $z^{-d^i} B_r^i(z^{-1}, k) u^i(k) / A_r^i(z^{-1}, k)$  denotes a linear time-varying dynamic system of the  $i$ th subsystem,  $\sum_{j=1, j \neq i}^n z^{-d_j^i} B_j^i(z^{-1}, k) u^j(k) / A_r^i(z^{-1}, k)$  stands for the interconnection stemming from the other subsystems,  $U(k) = [u^1(k) \ u^2(k) \ \dots \ u^n(k)]^T$ ,  $u^i(k)$  and  $y_p^i(k)$ ,  $i = 1, 2, \dots, n$  denote the system input and the system output of the  $i$ th subsystem, and  $\Delta^i(U(k), k)$  represents the nonlinear time-varying uncertainties.

In order to design an effective decentralized controller for an interconnected system,  $n$  dynamic models are required. The

pseudorandom binary signal (PRBS) with suitable amplitude and period is employed to drive each subsystem of the interconnected system at one time. Then the input and output pairs of data  $\{u^i(k), y_p^i(k)\}$ ,  $i = 1, 2, \dots, n$  are achieved. These input/output pairs are individually fed into the following least squares parameter estimation algorithm:

$$\hat{\theta}^i(k) = \hat{\theta}^i(k-1) + K^i(k-1) \times [y_p^i(k) - \phi^i(k-1)^T \hat{\theta}^i(k-1)] \quad (2a)$$

$$K^i(k-1) = P^i(k-1) \phi^i(k-1) \times [\gamma^i + \phi^i(k-1)^i P^i(k-1) \phi^i(k-1)]^{-1} \quad (2b)$$

$$P^i(k) = \frac{[I - K^i(k-1) \phi^i(k-1)^T] P^i(k-1)}{\gamma^i} \quad (2c)$$

$$\phi^i(k-1) = \begin{bmatrix} -y_p^i(k-1) & \dots & -y_p^i(k-n^i) \\ u^i(k-1) & \dots & u^i(k-m^i) \end{bmatrix}^T \quad (2d)$$

where  $1^- \leq \gamma^i \leq 1$ , the initial value of  $P^i(0) = \alpha^i I$ ,  $\alpha^i$  is large enough, the system degrees  $n^i$ ,  $m^i$  of the  $i$ th subsystem are chosen based on the prior knowledge of the subsystem. After the model verification, an appropriate learned model for the  $i$ th subsystem is expressed as follows:

$$y_p^i(k) = \frac{z^{-d^i} B^i(z^{-1}) u^i(k)}{A^i(z^{-1})}, \quad i = 1, 2, \dots, n \quad (3)$$

where the polynomials  $A^i(z^{-1})$  and  $B^i(z^{-1})$  for  $i = 1, 2, \dots, n$  are coprime. Then the interconnected system (1) is rewritten as the aforementioned subsystems with output disturbance  $d_o^i(k)$ ,  $i = 1, 2, \dots, n$

$$y_p^i(k) = \frac{z^{-d^i} B^i(z^{-1}) u^i(k)}{A^i(z^{-1})} + d_o^i(k) \quad (4a)$$

where

$$d_o^i(k) = \frac{\{z^{-d^i} B_r^i(z^{-1}, k) u^i(k) + \sum_{j=1, j \neq i}^n z^{-d_j^i} B_j^i(z^{-1}, k) u^j(k)\}}{A_r^i(z^{-1}, k)} + \Delta^i(U(k), k) - \frac{z^{-d^i} B^i(z^{-1}) u^i(k)}{A^i(z^{-1})}. \quad (4b)$$

The above output disturbance is relatively bounded as follows:

$$|d_o^i(k)| \leq \alpha_0^i + \sum_{j=1}^n \alpha_j^i |u^j(k-1)| \quad (4c)$$

where  $\alpha_0^i$  and  $\alpha_j^i$ ,  $i, j = 1, 2, \dots, n$  are bounded. In Section IV, the upper bound of  $\alpha_0^i$  and  $\alpha_j^i$ ,  $i, j = 1, 2, \dots, n$  is addressed for the stability of the closed-loop system.

The reference input to be tracked for the  $i$ th subsystem, i.e.,  $r^i(k)$  is assigned as follows:

$$Z\{r^i(k)\} = \frac{C_r^i(z^{-1})}{F_r^i(z^{-1})} \quad (5)$$

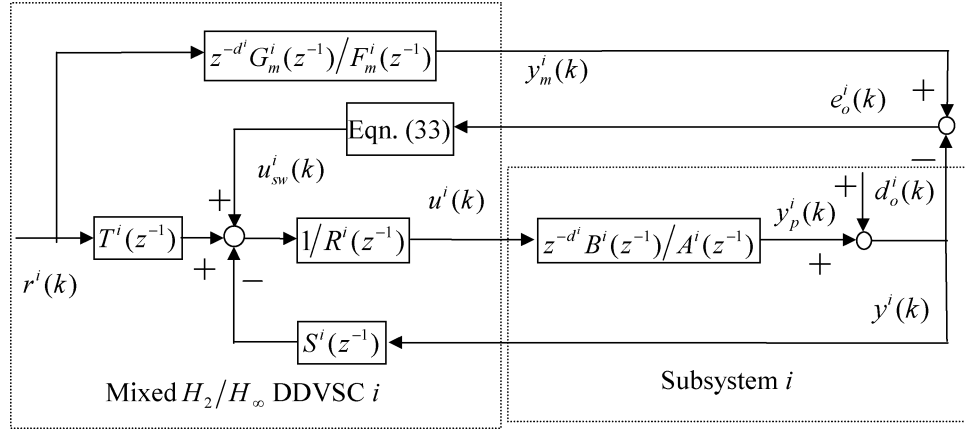


Fig. 1. Control block diagram of the  $i$ th subsystem.

where  $G_r^i(z^{-1})$  and  $F_r^i(z^{-1})$  for  $i = 1, 2, \dots, n$  are coprime. The proposed control of the  $i$ th subsystem is assumed as the following form (see Fig. 1):

$$R^i(z^{-1})u^i(k) = -S^i(z^{-1})y^i(k) + T^i(z^{-1})r^i(k) + u_{sw}^i(k) \quad (6a)$$

$$y^i(k) = y_p^i(k) + d_o^i(k) \quad (6b)$$

where  $d_o^i(k)$  is caused by the interactions, modeling error, and external load;  $y^i(k)$  denotes the feedback output of the  $i$ th subsystem; the polynomials  $R^i(z^{-1})$ ,  $S^i(z^{-1})$ , and  $T^i(z^{-1})$  are found to achieve an equivalent control of the  $i$ th subsystem; and  $u_{sw}^i(k)$  represents the switching control of the  $i$ th subsystem.

Assume that the input/output relationship between  $r^i(k)$  and  $y_m^i(k)$  for a stable reference model, is written as follows:

$$y_m^i(k) = \frac{z^{-d^i} G_m^i(z^{-1})}{F_m^i(z^{-1})} r^i(k) \quad (7)$$

where  $G_m^i(z^{-1})$  and  $F_m^i(z^{-1})$  for  $i = 1, 2, \dots, n$  are coprime, and  $F_m^i(z^{-1})$  is a stable monic polynomial with degree  $n_{f_m}^i$ . The purpose of using a reference model is to shape the response of the closed-loop system. Define the following output error of the  $i$ th subsystem:

$$e_o^i(k) = y_m^i(k) - y^i(k). \quad (8)$$

Then the response of  $e_o^i(k)$  from the inputs  $r^i(k)$ ,  $d_o^i(k)$ ,  $u_{sw}^i(k)$  is accomplished from (4), (6), (7), and (8), i.e.,

$$e_o^i(k) = L^i(z^{-1})r^i(k) - V^i(z^{-1})d_o^i(k) - D^i(z^{-1})u_{sw}^i(k) \quad (9a)$$

where

$$L^i(z^{-1}) = z^{-d^i} \left[ \frac{G_m^i(z^{-1})}{F_m^i(z^{-1})} - \frac{B^i(z^{-1})T^i(z^{-1})}{A_c^i(z^{-1})} \right] \quad (9b)$$

$$V^i(z^{-1}) = \frac{A^i(z^{-1})R^i(z^{-1})}{A_c^i(z^{-1})} \quad (9c)$$

$$D^i(z^{-1}) = \frac{z^{-d^i} B^i(z^{-1})}{A_c^i(z^{-1})}. \quad (9d)$$

The polynomial  $A_c^i(z^{-1})$  denotes the characteristic polynomial of the closed-loop system of the  $i$ th subsystem

$$A_c^i(z^{-1}) = A^i(z^{-1})R^i(z^{-1}) + z^{-d^i} B^i(z^{-1})S^i(z^{-1}). \quad (10)$$

For synthesizing the problem, two cost functions in the  $H_2$ -norm and  $H_\infty$ -norm spaces are defined as follows (e.g., see [10] and [11]):

$$J_1 = \left\| E_o^i(z^{-1}) + z^{-d^i} W_1^i(z^{-1})U^i(z^{-1}) \right\|_2$$

$$J_2 = \left\| W_2^i(z^{-1})V^i(z^{-1}) \right\|_\infty \quad (11)$$

where the weighted functions  $W_1^i(z^{-1})$  and  $W_2^i(z^{-1})$  denote two suitable rational functions;  $E_o^i(z^{-1})$  and  $z^{-d^i}U^i(z^{-1})$  are the pulse transfer functions of  $e_o^i(k)$  and  $u^i(k-d^i)$ , respectively.

The objectives of this paper are described as follows (cf. Fig. 1): 1) the equivalent control [i.e., the polynomials  $R^i(z^{-1})$ ,  $S^i(z^{-1})$ , and  $T^i(z^{-1})$ ] is obtained by the satisfaction of the following two requirements: a) For  $d_o^i(k) = u_{sw}^i(k) = 0$ , the cost function is  $J_1$  minimized; b) for  $u_{sw}^i(k) = 0$  the cost function  $J_2$  is simultaneously minimized; and 2) based on the Lyapunov redesign, the switching control (i.e.,  $u_{sw}^i(k)$ ) is designed to enhance system performance.

### III. MIXED $H_2/H_\infty$ DESIGN FOR DECENTRALIZED DISCRETE VARIABLE STRUCTURE CONTROL

There are three subsections for the mixed  $H_2/H_\infty$  design of decentralized discrete variable structure control (mixed  $H_2/H_\infty$  DDVSC).

#### A. Minimization of $J_1$

For  $d_o^i(k) = u_{sw}^i(k) = 0$ , the following results are obtained from Fig. 1.

$$U^i(z^{-1}) = \frac{A^i(z^{-1})T^i(z^{-1})G_r^i(z^{-1})}{[A_c^i(z^{-1})F_r^i(z^{-1})]} \quad (12)$$

$$E_o^i(z^{-1}) = z^{-d^i} \left[ \frac{G_m^i(z^{-1})}{F_m^i(z^{-1})} - \frac{B^i(z^{-1})T^i(z^{-1})}{A_c^i(z^{-1})} \right] \frac{G_r^i(z^{-1})}{F_r^i(z^{-1})}. \quad (13)$$

Substituting (5), (9), (12), and (13) into (11) yields (14), shown at bottom of page, where  $W_1^i(z^{-1}) = W_{1n}^i(z^{-1})/W_{1d}^i(z^{-1})$  and the zeros of monic polynomial  $W_{1d}^i(z^{-1})$  are in  $|z| < 1$ . Based on the norm-preserving property of the inner function, it is immediate from (14) that  $J_1$  is reduced to (15), shown at bottom of page. Let

$$W_{1d}^i(z^{-1})B^i(z^{-1}) - W_{1n}^i(z^{-1})A^i(z^{-1}) = C^i(z^{-1}) \quad (16)$$

where the polynomial of  $C^i(z^{-1})$  does not have zero on the unit circle. The following lemma gives the summary result of this section.

**Lemma 1:** The optimal controller for the cost function  $J_1$  is achieved from (10), (17), and (18), where  $F_o^i(z^{-1})$  is obtained from (A6) and takes the factorization of  $C^i(z^{-1})$  in (16) for an appropriate weighted function  $W_1^i(z^{-1})$

$$A_c^i(z^{-1}) = \bar{C}_-^i(z^{-1})\bar{G}_{r-}^i(z^{-1})C_+^i(z^{-1})G_{r+}^i(z^{-1}) \times F_m^i(z^{-1})X^i(z^{-1}) \quad (17)$$

$$T^i(z^{-1}) = W_{1d}^i(z^{-1})F_o^i(z^{-1})X^i(z^{-1}) \quad (18)$$

where  $X^i(z^{-1})$  is a stable polynomial. The corresponding minimum cost function  $J_1$  is given as (19).

$$J_{1\min} = \left\| \frac{F_c^i(z^{-1})}{C_-^i(z^{-1})} \right\|_2. \quad (19)$$

*Proof:* See Appendix A.

**Remark 1:** In fact, the coefficients of the polynomial  $F_o^i(z^{-1})$  are obtained from the following matrix equation:

$$\begin{bmatrix} 1 & z_1^i & \cdots & (z_1^i)^{-1+n_{fo}^i} \\ 1 & z_2^i & \cdots & (z_2^i)^{-1+n_{fo}^i} \\ \vdots & \vdots & \vdots & \vdots \\ 1 & z_{n_{fo}^i}^i & \cdots & (z_{n_{fo}^i}^i)^{-1+n_{fo}^i} \end{bmatrix} \begin{bmatrix} f_{o,0}^i \\ f_{o,1}^i \\ \vdots \\ f_{o,-1+n_{fo}^i}^i \end{bmatrix} = \begin{bmatrix} W^i(z_1^i) \\ W^i(z_2^i) \\ \vdots \\ W^i(z_{n_{fo}^i}^i) \end{bmatrix} \quad (20)$$

where

$$W^i(z^{-1}) = \bar{C}_-^i(z^{-1})\bar{G}_{r-}^i(z^{-1})G_m^i(z^{-1})G_{r+}^i(z^{-1})/C_-^i(z^{-1}).$$

**Remark 2:** The weighted function  $W_1^i(z^{-1})$  denotes frequency weighting (i.e.,  $|W_1^i(e^{-jwT_s})|$ ), where  $0 \leq w \leq \pi/T_s$ ) of control input. In general, a high-pass feature is assigned to attenuate the high-frequency response of control input.

## B. Minimization of $J_2$

In this subsection, the task is to find the polynomials  $R^i(z^{-1})$  and  $S^i(z^{-1})$  such that the optimal  $J_2$  is obtained. According to the concept of the previous papers (e.g., [18]), the optimal  $\|W_2^i(z^{-1})V^i(z^{-1})\|_\infty$  must satisfy the following interpolation constraints:

$$V^i(p_j^i) = 0, \quad j = 1, 2, \dots, n_{a-}^i \quad (21a)$$

$$1 - V^i(z_j^i) = 0, \quad j = 1, 2, \dots, n_{z_j}^i - 1 \quad (21b)$$

where  $n_{z_j}^i = n_{b-}^i + d^i$ ,  $p_j^i$  ( $1 \leq j \leq n_{a-}^i$ ) and  $z_j^i$  ( $1 \leq j \leq n_{z_j}^i - 1$ ) denote the zeros of  $A_-^i(z^{-1})$  and  $z^{-d^i}B_-^i(z^{-1})$ , respectively. Then the following lemma is given to explain the result of the minimax optimization.

**Lemma 2:**

1) The optimal  $J_2^* = [W_2^i(z^{-1})V^i(z^{-1})]^*$ , which minimizes  $\|W_2^i(z^{-1})V^i(z^{-1})\|_\infty$ , is of an all-pass form:

$$[W_2^i(z^{-1})V^i(z^{-1})]^* = \begin{cases} \frac{\rho^i \bar{\Phi}^i(z^{-1})}{\Phi^i(z^{-1})}, & \text{if } n_{z_j}^i = n_{\phi}^i + 1 \geq 1 \\ 0, & \text{if } n_{z_j}^i = 0 \end{cases}$$

where the polynomial  $\Phi^i(z^{-1})$  is monic and stable.

2) The constant  $\rho^i$  and  $\phi_j^i$  ( $1 \leq j \leq n_{\phi}^i$ ) are real and are uniquely determined by the interpolation constraints (21). Furthermore, the minimized  $\|W_2^i(z^{-1})V^i(z^{-1})\|_\infty$  is given by

$$\min \|W_2^i(z^{-1})V^i(z^{-1})\|_\infty = \left\| [W_2^i(z^{-1})V^i(z^{-1})]^* \right\|_\infty = |\rho^i|.$$

Based on the result of Lemma 2 and the constraint (21a), the following equation is achieved

$$V^i(z^{-1}) = \frac{\rho^i W_{2d}^i(z^{-1})A_-^i(z^{-1})\bar{\Phi}^i(z^{-1})}{[W_{2n}^i(z^{-1})\bar{A}_-^i(z^{-1})\Phi^i(z^{-1})]} \quad (22)$$

where  $W_{2n}^i(z^{-1}) = W_{2n}^i(z^{-1})/W_{2d}^i(z^{-1})$ ,  $W_{2n}^i(z^{-1})$  is a stable polynomial, and  $W_{2d}^i(z^{-1})$  contains the zeros on  $|z| \geq 1$  for rejecting the corresponding output disturbance (see Remark 3). Furthermore, the constraint (21b) gives the following result:

$$W_{2n}^i(z^{-1})\bar{A}_-^i(z^{-1})\bar{\Phi}^i(z^{-1}) - \rho^i W_{2d}^i(z^{-1})A_-^i(z^{-1})\bar{\Phi}^i(z^{-1}) = z^{-d^i}B_-^i(z^{-1})Q^i(z^{-1}) \quad (23)$$

$$J_1 = \left\| \frac{z^{-d^i} \{W_{1d}^i(z^{-1})[A_c^i(z^{-1})G_m^i(z^{-1}) - F_m^i(z^{-1})B^i(z^{-1})T^i(z^{-1})] + W_{1n}^i(z^{-1})A^i(z^{-1})T^i(z^{-1})F_m^i(z^{-1})\} G_r^i(z^{-1})}{W_{1d}^i(z^{-1})A_c^i(z^{-1})F_m^i(z^{-1})F_r^i(z^{-1})} \right\|_2 \quad (14)$$

$$J_1 = \left\| \frac{\{W_{1d}^i(z^{-1})[A_c^i(z^{-1})G_m^i(z^{-1}) - F_m^i(z^{-1})B^i(z^{-1})T^i(z^{-1})] + W_{1n}^i(z^{-1})A^i(z^{-1})T^i(z^{-1})F_m^i(z^{-1})\} G_r^i(z^{-1})}{W_{1d}^i(z^{-1})A_c^i(z^{-1})F_m^i(z^{-1})F_r^i(z^{-1})} \right\|_2 \quad (15)$$

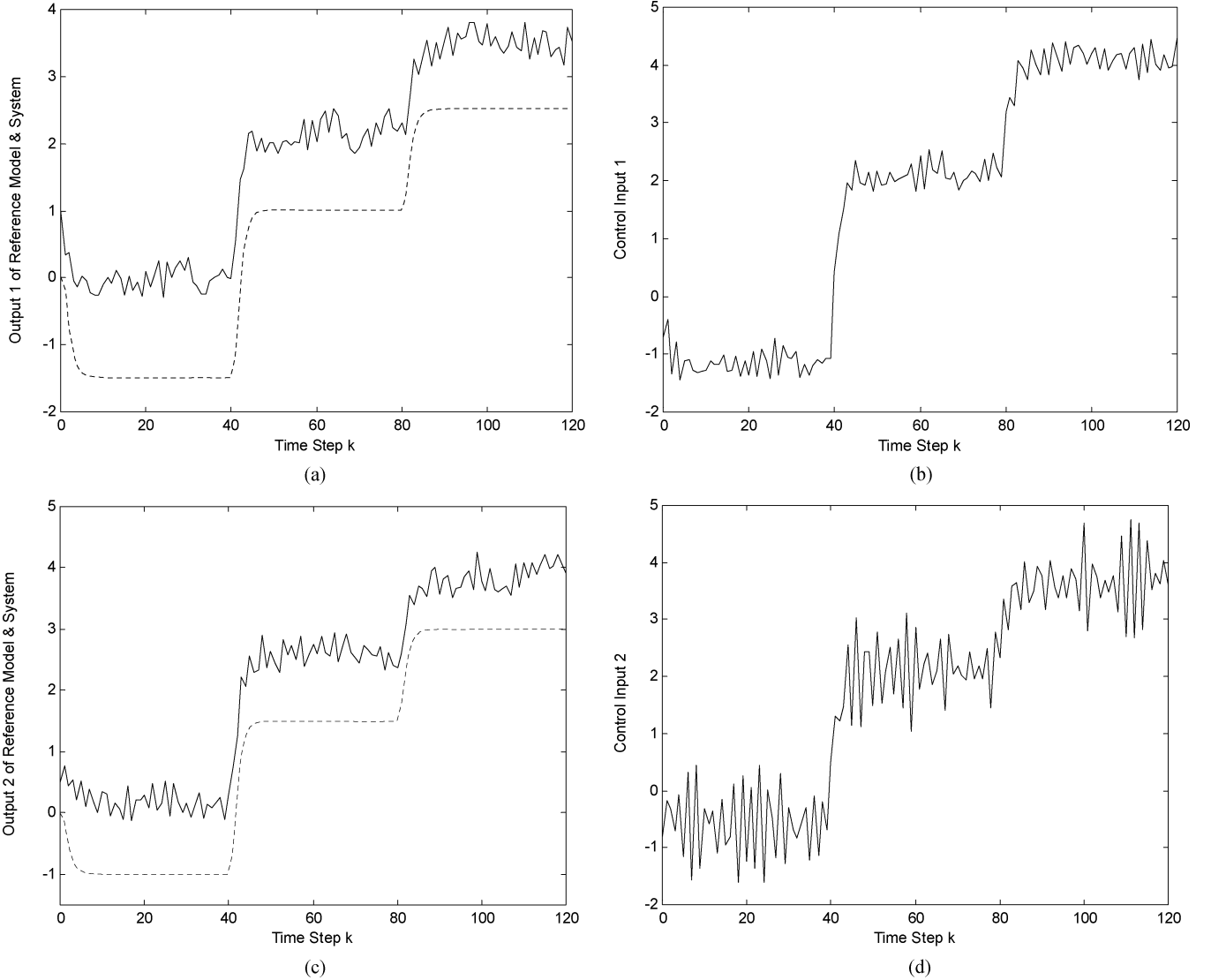


Fig. 2. Response for the controller design only based on  $H_2$ -optimization with  $W_1^i(z^{-1}) = W_{11}(z^{-1})$ . (a)  $y_m^1(k)(\cdots)$  and  $y^1(k)(-)$ . (b)  $u^1(k)$ . (c)  $y_m^2(k)(\cdots)$  and  $y^2(k)(-)$ . (d)  $u^2(k)$ .

where  $n_\phi^i = d^i + n_{b-}^i - 1$  and  $n_q^i = n_{w_{2n}}^i + n_{a-}^i - 1$ . Or, rewrite (23) as

$$W_{2n}^i(z_j^i) \bar{A}_-(z_j^i) \Phi^i(z_j^i) - \rho^i W_{2d}^i(z_j^i) A_-^i(z_j^i) \bar{\Phi}^i(z_j^i) = 0. \quad (24)$$

By the solution of  $\rho^i$  and  $\bar{\Phi}^i(z^{-1})$  from (24), the following equations are accomplished from (9c), (22), and (23)

$$A_c^i(z^{-1}) = A_+^i(z^{-1}) W_{2n}^i(z^{-1}) \bar{A}_-(z^{-1}) \Phi^i(z^{-1}) \times B_+^i(z^{-1}) \hat{X}^i(z^{-1}) \quad (25)$$

$$R^i(z^{-1}) = \rho^i W_{2d}^i(z^{-1}) \bar{\Phi}^i(z^{-1}) B_+^i(z^{-1}) \tilde{X}^i(z^{-1}). \quad (26)$$

Comparing (25) and (17) gives

$$\tilde{X}^i(z^{-1}) = \bar{C}_-(z^{-1}) \bar{G}_{r-}^i(z^{-1}) C_+^i(z^{-1}) G_{r+}^i(z^{-1}) \times F_m^i(z^{-1}) \hat{X}^i(z^{-1}) \quad (27)$$

$$X^i(z^{-1}) = B_+^i(z^{-1}) A_+^i(z^{-1}) W_{2n}^i(z^{-1}) \bar{A}_-(z^{-1}) \times \Phi^i(z^{-1}) \hat{X}^i(z^{-1}) \quad (28)$$

where  $\hat{X}^i(z^{-1})$  is a stable polynomial. Then from (25)–(28)

$$A_c^i(z^{-1}) = \bar{C}_-(z^{-1}) \bar{G}_{r-}^i(z^{-1}) C_+^i(z^{-1}) G_{r+}^i(z^{-1}) \times F_m^i(z^{-1}) B_+^i(z^{-1}) A_+^i(z^{-1}) W_{2n}^i(z^{-1}) \times \bar{A}_-(z^{-1}) \Phi^i(z^{-1}) \hat{X}^i(z^{-1}) \quad (29)$$

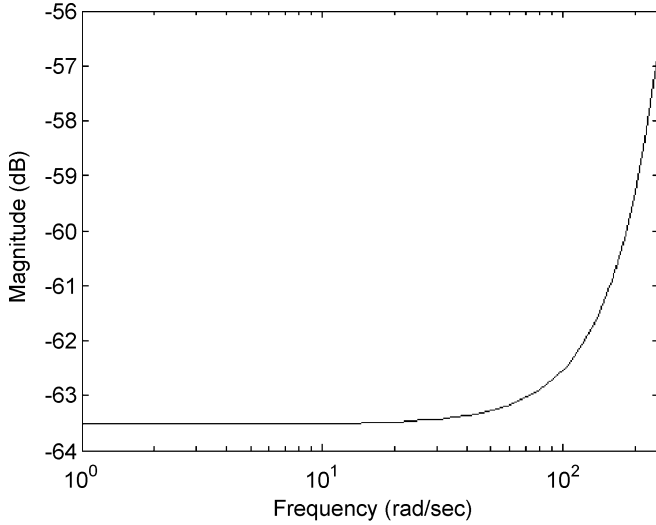
$$R^i(z^{-1}) = \rho^i W_{2d}^i(z^{-1}) \bar{\Phi}^i(z^{-1}) B_+^i(z^{-1}) \bar{C}_-(z^{-1}) \times \bar{G}_{r-}^i(z^{-1}) C_+^i(z^{-1}) G_{r+}^i(z^{-1}) \times F_m^i(z^{-1}) \hat{X}^i(z^{-1}). \quad (30)$$

Substituting the relations (28), (29), and (23) into (10) yields

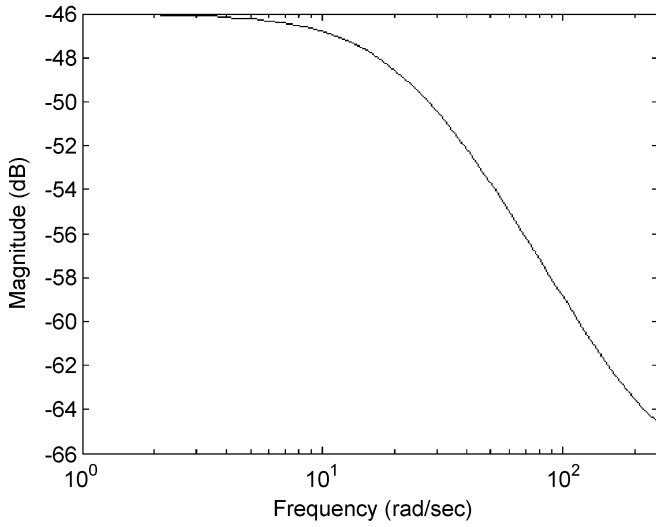
$$S^i(z^{-1}) = A_+^i(z^{-1}) Q^i(z^{-1}) \bar{C}_-(z^{-1}) \bar{G}_{r-}^i(z^{-1}) C_+^i(z^{-1}) \times G_{r+}^i(z^{-1}) F_m^i(z^{-1}) \hat{X}^i(z^{-1}). \quad (31)$$

From (18) and (28), the polynomial  $T^i(z^{-1})$  is attained as follows:

$$T^i(z^{-1}) = W_{1d}^i(z^{-1}) F_o^i(z^{-1}) B_+^i(z^{-1}) A_+^i(z^{-1}) W_{2n}^i(z^{-1}) \times \bar{A}_-(z^{-1}) \Phi^i(z^{-1}) \hat{X}^i(z^{-1}). \quad (32)$$



(a)



(b)

Fig. 3. Frequency responses of  $W_1^i(z^{-1}) = W_{11}(z^{-1})$  and  $W_2^i(z^{-1}) = W_{12}(z^{-1})$ . (a)  $W_1^1(z^{-1}) = W_{11}(z^{-1})$ . (b)  $W_1^2(z^{-1}) = W_{12}(z^{-1})$ .

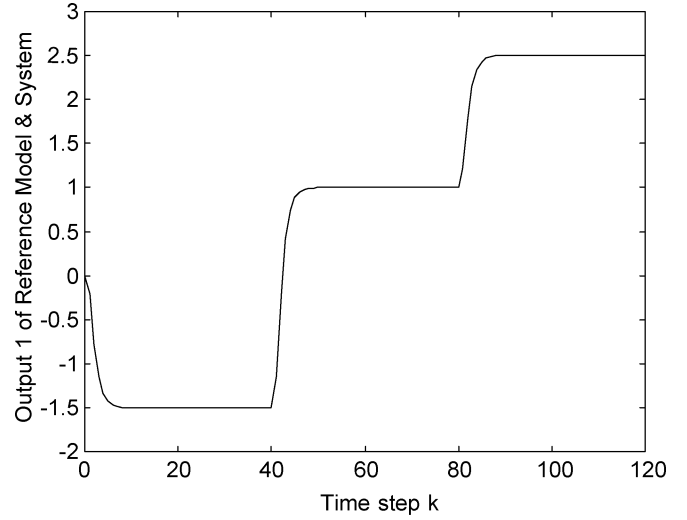
That is, the control polynomials  $\{R^i(z^{-1}), S^i(z^{-1}), T^i(z^{-1})\}$  for the mixed  $H_2/H_\infty$  optimization in (11) are attained from (30)–(32).

*Remark 3:* To reject the output disturbance, the polynomial  $W_{2d}^i(z^{-1})$  must contain the corresponding modes. For example,  $W_{2d}^2(z^{-1}) = (1 - z^{-1})(1 - 2 \cos(\omega^i T_s)z^{-1} + z^{-2})$  is used for rejecting the output disturbance  $d_o^i(k) = K_1^i + K_2^i \sin(\omega^i t + \phi^i)$ , where  $K_1^i$ ,  $K_2^i$  and  $\phi^i$  are unknown but bounded constants. In general, an all-pass feature with infinity dc gain is assigned to reject an output disturbance including a constant and the other frequencies.

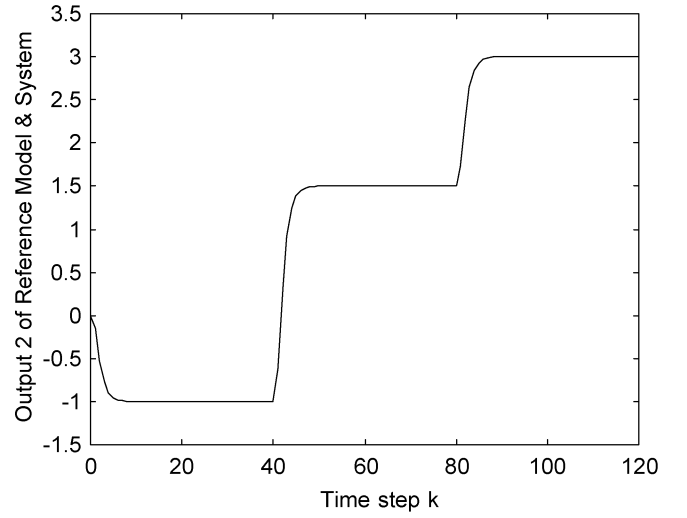
### C. Switching Control for Enhanced Robustness

The proposed switching control is designed as follows:

$$u_{sw}^i(k) = \begin{cases} -\frac{A_c^i(z^{-1})[e_o^i(k) + v_{sw}^i(k)]}{[B_+^i(z^{-1})\bar{B}_-^i(z^{-1})]}, & \text{if } |e_o^i(k)| > \chi^i(k) \\ 0, & \text{otherwise} \end{cases} \quad (33)$$



(a)



(b)

Fig. 4. Output response of mixed  $H_2/H_\infty$  control for  $d_o^i = 0$ ,  $i = 1, 2$  with the weighted functions  $W_1^i(z^{-1}) = W_{11}(z^{-1})$ ,  $i = 1, 2$ ,  $W_2^1(z^{-1}) = W_{21}(z^{-1})$ , and  $W_2^2(z^{-1}) = W_{22}(z^{-1})$ . (a)  $y_m^1(k)$ ( $\cdots$ ) and  $y^1(k)$ ( $-$ ). (b)  $y_m^2(k)$ ( $\cdots$ ) and  $y^2(k)$ ( $-$ ).

where  $A_c^i(z^{-1})$  is the same as (29),  $v_{sw}^i(k)$  is given in (42), and  $\chi^i(k)$  is described in (43). Substituting (33), (9c), and (10) into (9a) gives

$$e_o^i(k) = L^i(z^{-1})^* r^i(k) + V^i(z^{-1})^* d_o^i(k) + \frac{B_-^i(z^{-1}) [e_o^i(k - d^i) + v_{sw}^i(k - d^i)]}{\bar{B}_-^i(z^{-1})} \quad (34)$$

where  $L^i(z^{-1})^*$  and  $V^i(z^{-1})^*$  are the rational functions corresponding to the optimal cost functions  $J_1^*$  and  $J_2^*$ , respectively. Based on the facts in (4), the signal  $V^i(z^{-1})^* d_o^i(k)$  in (34) contains the effect of the switching control of the  $i$ th subsystem, i.e.,  $v_{sw}^i(k - d^i)$ . It must be decomposed into two parts for the stability analysis: one includes  $v_{sw}^i(k - d^i)$  and the other is without it. From (4b), (6), and (7), the following equation is assumed to be true.

$$V^i(z^{-1})^* d_o^i(k) = \gamma_{11}^i(k) v_{sw}^i(k - d^i) + \sum_{j=1}^n \gamma_{2j}^i(k) e_o^j(k - d^j) + \gamma_3^i(k) \quad (35)$$

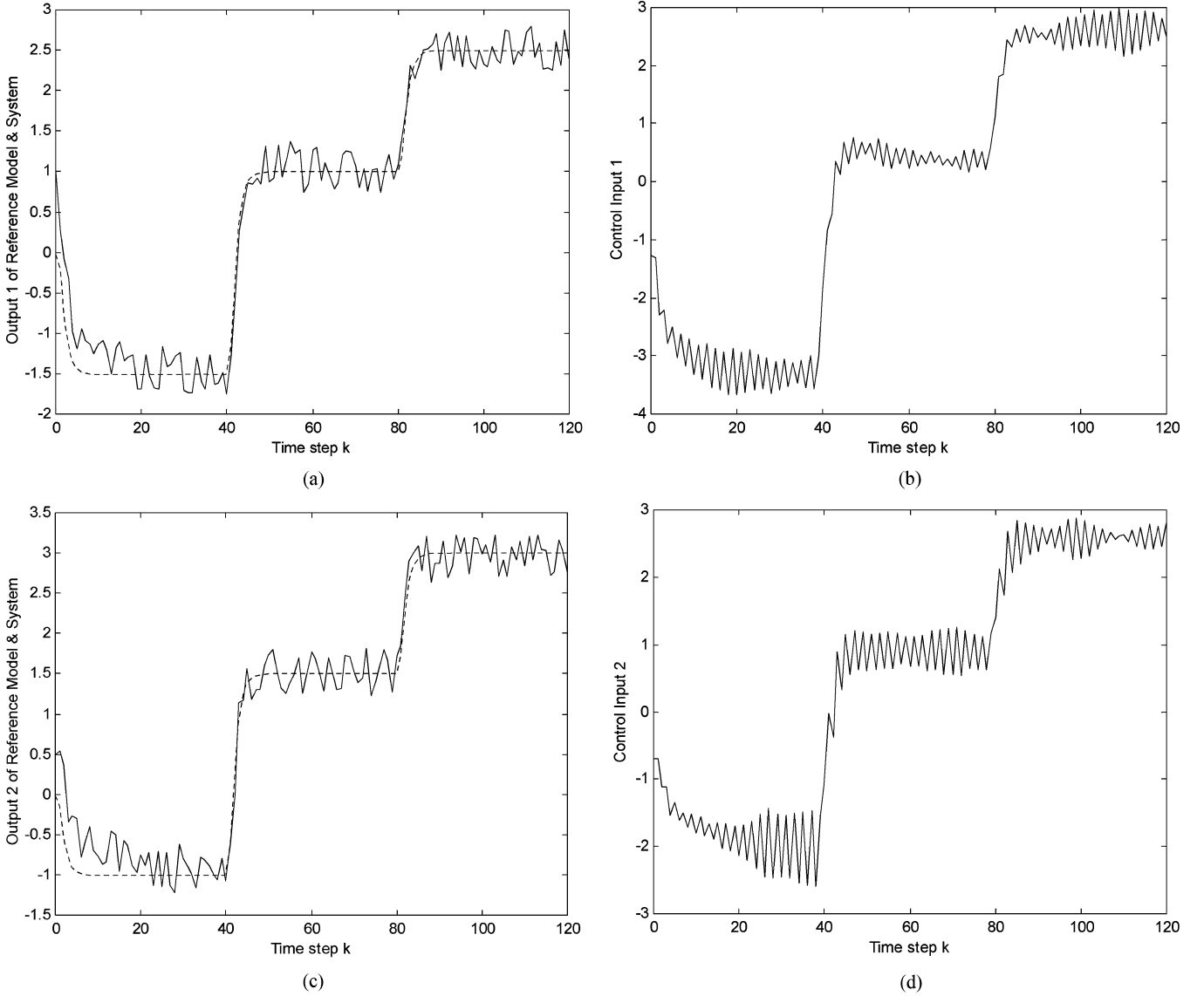


Fig. 5. Response for Fig. 4 case except  $d_o^1(k)$  and  $d_o^2(k)$  in (50a) and (50b). (a)  $y_m^1(k)$  and  $y^1(k)$ . (b)  $u^1(k)$ . (c)  $y_m^2(k)$  and  $y^2(k)$ . (d)  $u^2(k)$ .

where  $|\gamma_1^i(k)| < \delta_1^i < 1$ ,  $|\gamma_{2j}^i(k)| < \delta_{2j}^i$ ,  $|\gamma_3^i(k)| < \delta_3^i$ ,  $\forall k$ , and  $i, j = 1, 2, \dots, n$ . Define the difference of  $e_o^i(k)$  as follows:

$$\Delta e_o^i(k) = e_o^i(k + d^i) - e_o^i(k). \quad (36)$$

Then from (34), (35), and (36)

$$\Delta e_o^i(k) = \Lambda^i(k) + [1 - \tau^i(z^{-1}, k)] v_{sw}^i(k) \quad (37)$$

where

$$\tau^i(z^{-1}, k) = 1 - \frac{B_i^-(z^{-1})}{\bar{B}_i^-(z^{-1})} - \gamma_1^i(k + d^i) \quad (38)$$

$$\begin{aligned} \Lambda^i(k) = & L^i(z^{-1}) * \tau^i(k + d^i) \\ & + \left\{ \gamma_{2i}^i(k + d^i) + \frac{[B_i^-(z^{-1}) - \bar{B}_i^-(z^{-1})]}{\bar{B}_i^-(q^{-1})} \right\} e_o^i(k) \\ & + \sum_{j=1, j \neq i}^n \gamma_{2j}^i(k + d^i) e_o^j(k - d^j + d^i) + \gamma_3^i(k + d^i). \end{aligned} \quad (39)$$

The upper bound of  $\Lambda^i(k)$  is estimated as follows:

$$|\Lambda^i(k)| \leq g_\lambda^i(k) = \lambda_0^i |e_o^i(k)| + \sum_{j=1, j \neq i}^n \lambda_{1j}^i |e_o^j(k)| + \lambda_2^i \quad (40)$$

where  $\lambda_{1j}^i \geq 0$ ,  $[(1 - \lambda^i)^2 - \varepsilon^j(1 + \lambda^i)^2]/[4(1 + \lambda^i)] > \lambda_0^i \geq 0$ ,  $1 > (1 - \lambda^i)^2/1 + \lambda^i > \varepsilon^i > 0$ ,  $1 > \lambda^i = \delta_1^i + v^i$ , satisfying the following inequality:

$$\left\| 1 - \frac{B_i^-(z^{-1})}{\bar{B}_i^-(z^{-1})} \right\|_\infty \leq v^i < 1, \text{ on } D^i \quad (41)$$

where  $D^i = \{z \in \mathbb{C} \mid |z| < 1\}$  is the domain containing the zeros of  $\bar{B}_i^-(z^{-1})$ . The control in (42) is then employed to deal with the unmodeled dynamics  $\Lambda^i(k)$ .

$$\begin{cases} v_{sw}^i(k) = -\frac{\xi^i(k) g_\lambda^i(k) e_o^i(k)}{[(1 - \lambda^i)(1 + \lambda^i)] |e_o^i(k)|}, & \text{if } |e_o^i(k)| > \chi^i(k) \\ u_{sw}^i(k) = 0, & \text{otherwise} \end{cases} \quad (42)$$

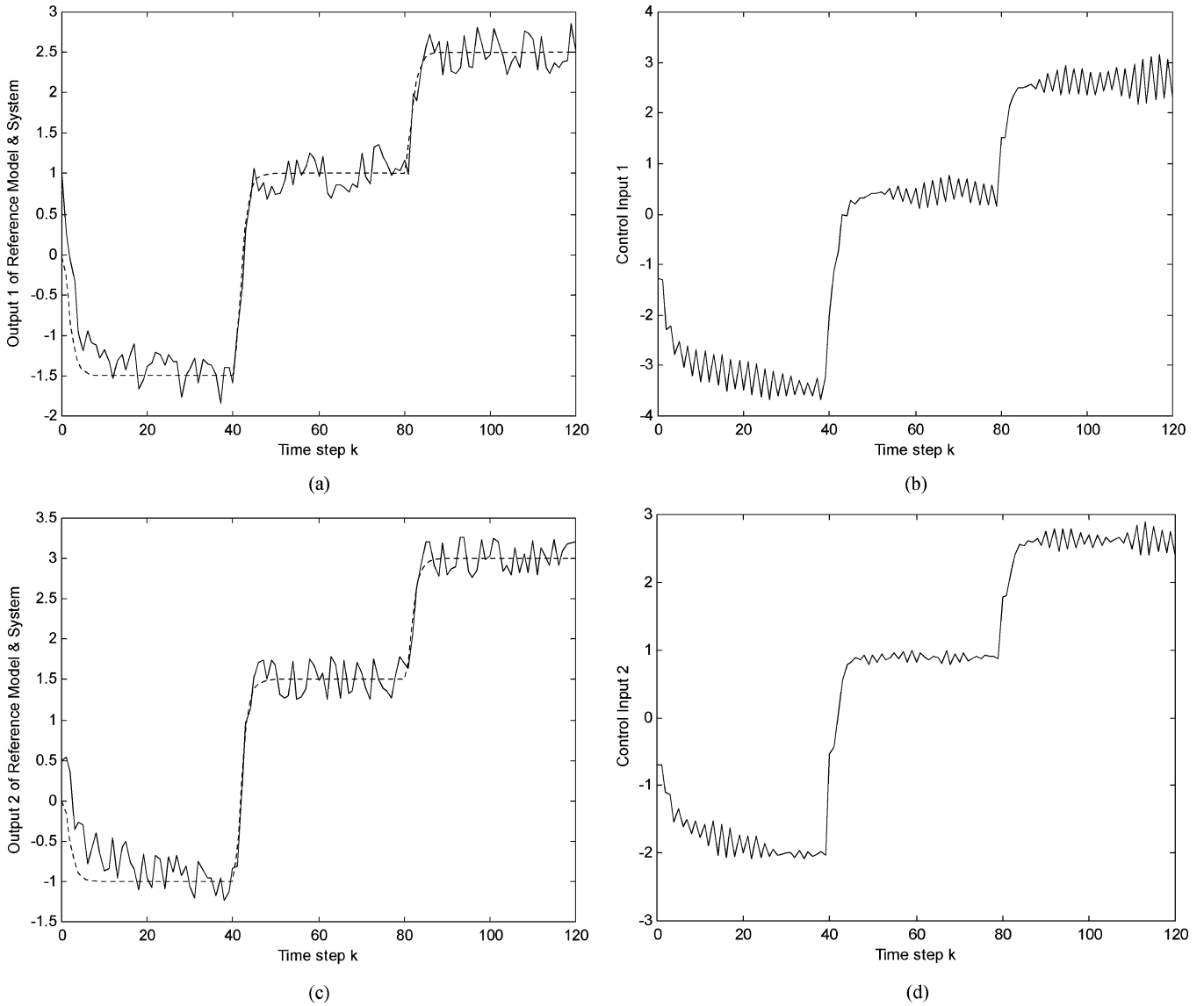


Fig. 6. Response of Fig. 5 case except  $W_1^i(z^{-1}) = W_{13}(z^{-1})$ ,  $i = 1, 2$ . (a)  $y_m^1(k)$ ( $\cdots$ ) and  $y^1(k)$ ( $-$ ). (b)  $u^1(k)$ . (c)  $y_m^2(k)$ ( $\cdots$ ) and  $y^2(k)$ ( $-$ ). (d)  $u^2(k)$ .

where

$$\chi^i(k) = \max \left\{ \frac{4(1 + \lambda^i) \left( \sum_{j=1, j \neq i}^n \lambda_{1j}^i |e_o^j(k)| + \lambda_2^i \right)}{\left[ (1 - \lambda^i)^2 - \varepsilon^i (1 + \lambda^i)^2 - 4(1 + \lambda^i) \lambda_0^i \right]}, \frac{4(1 + \lambda^i) g_\lambda^i(k)}{\left[ (1 - \lambda^i)^2 - \varepsilon^i (1 + \lambda^i)^2 \right]} \right\}. \quad (43)$$

The switching gain in (42) satisfies the following inequality:

$$\xi_2^i(k) > \xi^i(k) > \xi_1^i(k) \geq 0 \quad (44)$$

where

$$\xi_{1,2}^i(k) = g_1^i(k) \mp \sqrt{[g_1^i(k)]^2 - g_2^i(k)} \quad (45)$$

$$g_1^i(k) = \frac{(1 - \lambda^i)^2 |e_o^i(k)|}{\left[ (1 + \lambda^i) g_\lambda^i(k) \right] - (1 - \lambda^i)} \quad (46)$$

$$g_2^i(k) = \frac{(1 - \lambda^i)^2 \left\{ [g_\lambda^i(k)]^2 + 2g_\lambda^i(k) |e_o^i(k)| + \varepsilon^i |e_o^i(k)|^2 \right\}}{[g_\lambda^i(k)]^2}. \quad (47)$$

**Theorem 1:** Consider the system (4) and the controller (6) with  $u_{sw}^i(k)$  in (33) and  $v_{sw}^i(k)$  in (42). The polynomials  $R^i(z^{-1})$ ,  $S^i(z^{-1})$  and  $T^i(z^{-1})$  are achieved from (30)–(32). The inequalities in (40) and (41) are satisfied. Then  $\{u^i(k)\}$  is bounded,  $\{e_o^i(k)\}$  is bounded in the sense of the minimal  $J_1^*$  and  $J_2^*$ , and the following performance (48) is accomplished.

$$D_o = \{e_o^i(k) : |e_o^i(k)| \leq \chi^i(k)\}. \quad (48)$$

*Proof:* See Appendix B.

**Remark 4:** If the upper bound of the system uncertainties (40) [i.e.,  $g_\lambda^i(k)$ ] or the uncertainty of control gain (41) (i.e.,  $\lambda^i$ ) is large, the size of dead-zone  $\chi^i(k)$  in (43) will be large. To preserve the stability, the switching control shuts off as the

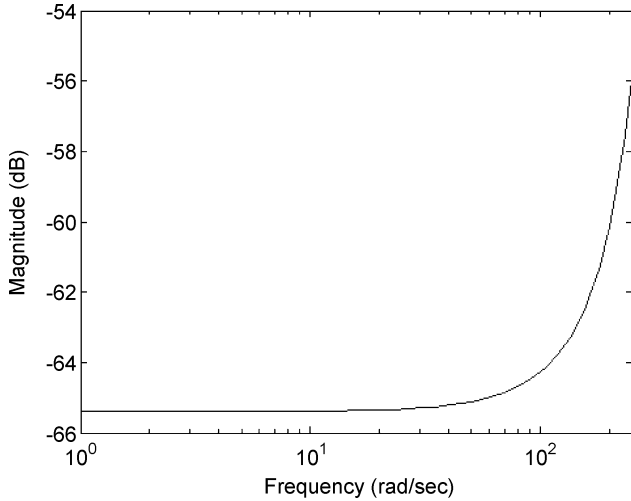


Fig. 7. Frequency response of  $W_1^i(z^{-1}) = W_{13}(z^{-1})$ .

operating point is in a larger  $|\sigma^i(k)|$ . In fact, the upper bound of system uncertainties (40) is limited by the inequality  $[(1 - \lambda^i)^2 - \varepsilon^i(1 + \lambda^i)^2]/[4(1 + \lambda^i)] > \lambda_0^i \geq 0$ . In addition, the system performance is less acceptable if  $\chi^i(k)$  becomes large [refer to (48)]. The tracking performance is expressed in (48), which indicates the performance of the  $i$ th subsystem is relatively bounded by the output error of the other subsystems. It also implies that any one subsystem is unstable then the interconnected system (1) is unstable. In this situation, from (35) and (4c) the upper bound of output disturbance must have a limit to ensure the stability of the closed-loop system.

#### IV. SIMULATION AND DISCUSSION

This section will give a comparison for the controller design based on only  $H_2$ -optimization, mixed  $H_2/H_\infty$ -optimization, and the proposed control. Assume that two nominal linear models for two subsystems are described as follows:

$$A^i(z^{-1}) = 1 + a_1^i z^{-1} + a_2^i z^{-2}$$

$$B^i(z^{-1}) = b_0^i + b_1^i z^{-1}, \quad d^i = 1, \quad i = 1, 2 \quad (49a)$$

$$a_1^1 = -0.378 \quad a_2^1 = 0.335$$

$$b_0^1 = 0.216 \quad b_1^1 = 0.432 \quad (49b)$$

$$a_1^2 = -0.663 \quad a_2^2 = 0.495$$

$$b_0^2 = 0.255 \quad b_1^2 = 0.459. \quad (49c)$$

These two subsystems are stable and in nonminimum phase. The desired trajectory is supposed to be the following form:  $r^1(k) = -1.5$ ,  $r^2(k) = -1$ , as  $0 \leq k < 40$ ;  $r^1(k) = 1$ ,  $r^2(k) = 1.5$ , as  $40 \leq k < 80$ ; and  $r^1(k) = 2.5$ ,  $r^2(k) = 3$ , as  $80 \leq k < 120$ . The output disturbances for these two subsystems are assumed as follows:

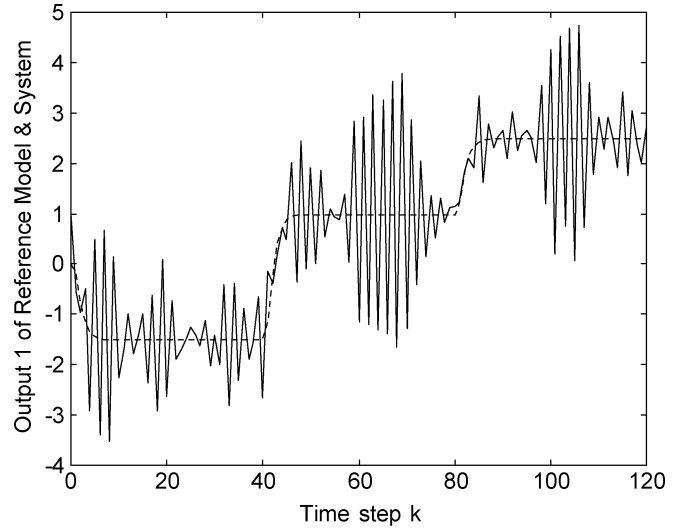
$$d_o^1(k) = 0.75 + 0.25 \cos(2\pi f_1^1 k T_s u^2(k-1))$$

$$- 0.2u^1(k-1) \sin(2\pi f_2^1 k T_s) \quad (50a)$$

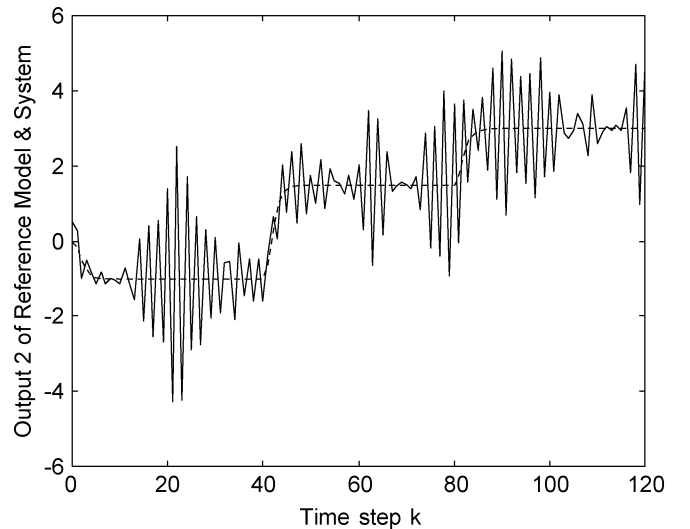
$$d_o^2(k) = 0.75 - 0.25 \cos(2\pi f_1^2 k T_s u^1(k-1))$$

$$+ 0.2u^2(k-1) \sin(2\pi f_2^2 k T_s) \quad (50b)$$

where  $f_1^1 = f_1^2 = 60$  Hz,  $f_2^1 = f_2^2 = 150$  Hz, and  $T_s = 0.01$  s. The reference models are supposed to be



(a)



(b)

Fig. 8. Output response of Fig. 6 case except  $W_2^1(z^{-1}) = W_{23}(z^{-1})$  and  $W_2^2(z^{-1}) = W_{24}(z^{-1})$ . (a)  $y_m^1(k)$ ( $\cdots$ ) and  $y^1(k)$ ( $-$ ). (b)  $y_m^2(k)$ ( $\cdots$ ) and  $y^2(k)$ ( $-$ ).

$G_m^1(z^{-1})/F_m^1(z^{-1}) = 0.14(1 + 2z^{-1})/(1 - 0.7z^{-1} + 0.12z^{-2})$ ,  $G_m^2(z^{-1})/F_m^2(z^{-1}) = 0.15(1 + 1.8z^{-1})/(1 - 0.7z^{-1} + 0.12z^{-2})$  which contain well-damped poles and unit static gain. In the beginning, only the  $H_2$ -optimization with the weighted function  $W_1^i(z^{-1}) = W_{11}(z^{-1}) = 0.001/(1 + 0.5z^{-1})$ ,  $i = 1, 2$  is used to obtain the controller (see Lemma 1). The corresponding response is depicted in Fig. 2, which is poor. More serious, an inappropriate selection of this weighted function will bring about instability; for instance, the response for the weighted function  $W_1^i(z^{-1}) = W_{12}(z^{-1}) = 0.001/(1 - 0.8z^{-1})$ ,  $i = 1, 2$ , diverges quickly; for simplicity, it is omitted. The reason is explained by Fig. 3, which represents the frequency responses of  $|W_{11}(e^{-j\omega T_s})|$  and  $|W_{12}(e^{-j\omega T_s})|$  where  $0 \leq \omega \leq \pi/T_s$  and  $T_s = 0.01$  sec. Because  $|W_{12}(e^{-j\omega T_s})|$  is a low-pass weighted function, the reduction of high-frequency component of the control input contaminated by the output disturbance is small.

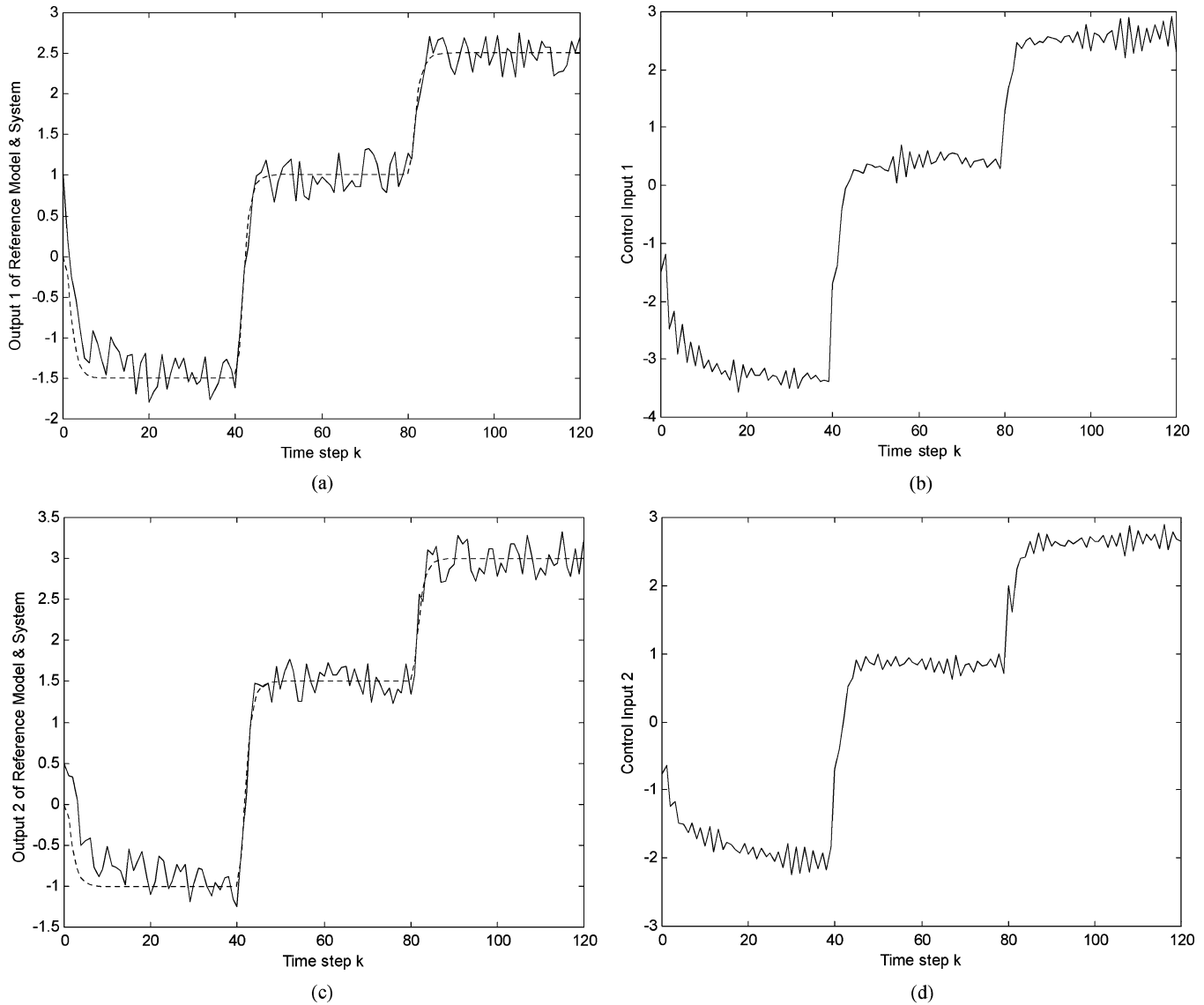


Fig. 9. Response of Fig. 6 case based on mixed  $H_2/H_\infty$  DDVSC. (a)  $y_m^1(k)$ ( $\cdots$ ) and  $y^1(k)$ ( $-$ ). (b)  $u^1(k)$ . (c)  $y_m^2(k)$ ( $\cdots$ ) and  $y^2(k)$ ( $-$ ). (d)  $u^2(k)$ .

On the contrary, the frequency response of  $|W_{11}(e^{-j\omega T_s})|$  is a high-pass weighted function which can effectively attenuate the high-frequency component of the control input. Although the controller design in Lemma 1 intends to minimize the energy consumption and output error, a large constant output disturbance deteriorates system performance much. It indicates that the controller design must deal with the situation often occurs and is important. According to on the above requirement, the controller design based on the mixed  $H_2/H_\infty$  technique is employed to deal with the system (49) in the face of the output disturbance (50).

In the beginning, the design of mixed  $H_2/H_\infty$  control is evaluated for  $d_o^i = 0, i = 1, 2$ . Besides  $W_1^i(z^{-1}) = W_{11}(z^{-1}), i = 1, 2$  the second weighted functions are set as follows:  $W_2^1(z^{-1}) = W_{21}(z^{-1}) = (0.8 - 0.72z^{-1})/(1 - z^{-1})$  and  $W_2^2(z^{-1}) = W_{22}(z^{-1}) = (1 - 0.92z^{-1})/(1 - z^{-1})$  which possess all-pass features with infinity dc gain. Then the corresponding response is shown in Fig. 4, which are excellent. Similarly, Fig. 5 depicts the response of Fig. 4

case except that the system is in the face of the output disturbance (50). It reveals that suitable weighted functions can obtain an acceptable performance. For reducing the high-frequency component of the control input, the weighted function  $W_1^i(z^{-1}) = W_{13}(z^{-1}) = 0.001/(1 + 0.8z^{-1})$  is applied to replace  $W_1^i(z^{-1}) = W_{11}(z^{-1}), i = 1, 2$ . The corresponding response is shown in Fig. 6, which indeed possesses smaller high-frequency response of the control input as compared with that in Fig. 4. Fig. 3(a) and Fig. 7 assert the corresponding result. In addition, the output responses of Figs. 5 and 6 are similar. In short, a suitable  $W_1^i(z^{-1}) = W_{13}(z^{-1})$  with more weight in high-frequency range can attenuate high-frequency component of control input. Furthermore, unsuitable second weighted functions, e.g.,  $W_2^1(z^{-1}) = W_{23}(z^{-1}) = (0.8 + 0.72z^{-1})/(1 - z^{-1})$  and  $W_2^2(z^{-1}) = W_{24}(z^{-1}) = (1 + 0.92z^{-1})/(1 - z^{-1})$  those have low-pass feature, can not attenuate the effect of high-frequency of the output disturbance (see Fig. 8). The responses of the control input are also chattering.

To improve robust performance and stability, the mixed  $H_2/H_\infty$  DDVSC with the control parameters  $\lambda_0^i = 0.001$ ,  $\lambda_{11}^i = \lambda_{12}^i = \lambda_2^i = 0.001$ ,  $\varepsilon^1 = 0.85$ ,  $\varepsilon^2 = 0.85$ ,  $\lambda^i = 0.001$  and  $\xi^i(k) = \xi_1^i(k) + 1.25g_1^i(k)\{1 - 0.995e^{-1000|e_o^i(k)|}\}$  is applied to the system (49) with the output disturbance (50). The corresponding response for Fig. 6 case is shown in Fig. 9. Comparison between Fig. 6(b) and (d) and Fig. 9(b) and (d) confirms that the switching control indeed improves the response of the control input. The output responses between Fig. 6(a) and (c) and Fig. 9(a) and (c) are almost the same. Because the output disturbance is immediately and randomly added into the system output, they can not immediately eliminate and attenuate by the control input. On the contrary, the sequences  $\{U(k-1), U(k-2), \dots, Y(k), Y(k-1), \dots\}$  are applied to the controller to calculate the control input  $U(k)$  which is improved by the switching control. In summary, the switching control is not necessarily to result in a chattering control input; on the contrary, a simultaneous enhancement of the control input and tracking accuracy is achieved. It is different from the results of traditional variable structure control (e.g., [12]–[14]).

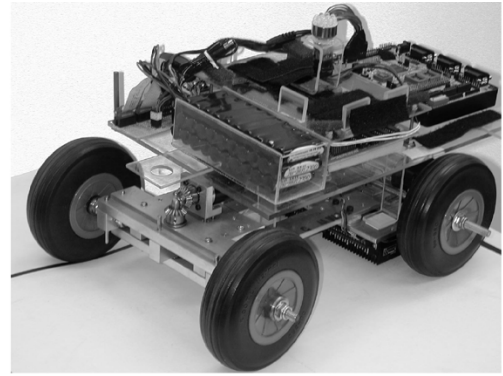
From the above analysis, the advantages of the mixed  $H_2/H_\infty$  DDVSC are given as follows.

- 1) The mixed  $H_2/H_\infty$  DDVSC for the interconnected system is simple because the system identification and the controller design of every subsystem are individually obtained.
- 2) A suitable selection of weighted functions influences system performance much. However, the switching control can further enhance robust stability and performance.

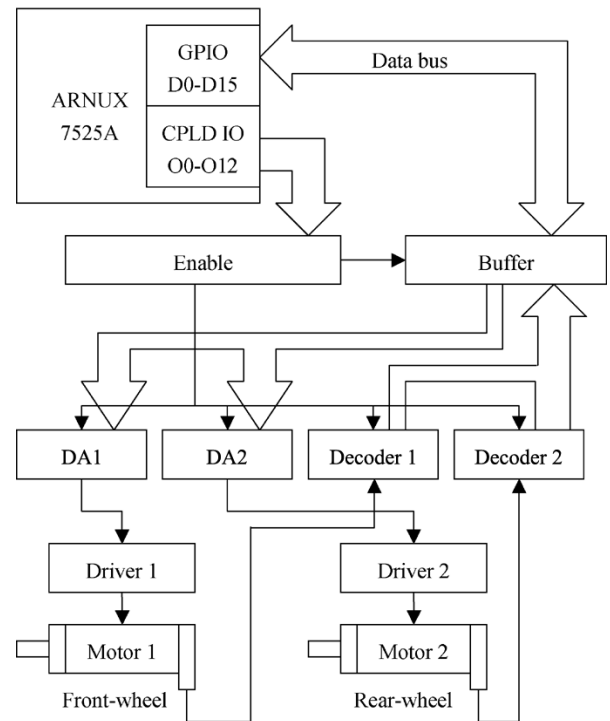
## V. APPLICATION TO MOBILE ROBOT

### A. Experimental Setup

Consider the car-like mobile robot (CLMR) with two wheels driving system in Fig. 10. The rear wheels are fixed parallel to the car chassis and allowed to roll or spin but not slip; two front wheels are parallel and can simultaneously turn to the right or left. The system hardware includes two dc motors, one microprocessor, one expansion circuit I/O card, one LED (Light Emitter Diode), and mechanism. In order to simulate the behaviors of a real car, we adopt the mobile robot with front steering wheels and rear-wheel drive as the chassis mechanism of the CLMR. Front-wheel and rear-wheel are individually driven by the same permanent magnet dc motor (i.e., A-max32 motor of Maxon Co.). The only difference is the gear ratio; one is 190:1, and the other is 51:1. Table I shows the basic specifications of the CLMR. In this paper, the core of CLMR is the microprocessor with Embedded Linux Platform ARNUX 7525A. This platform provides fully fledged Linux development environment by leveraging the generous, free, and open-sources in Linux world. In addition, the circuit expansion I/O card integrates three different circuits: 12-bit D/A Converter (AD7541A), 16-bit Decoder (HCTL2020), and 8-bit A/D converter (ADC0804). There are two DACs, two decoders, and eight ADCs in this expansion circuit I/O card. One LED is applied to estimate the position of the CLMR by one CCD in the height of 2540 mm. In order to design an effective decentralized controller for a CLMR, two dynamic models



(a)



(b)

Fig. 10. Experimental setup of the CLMR. (a) Photograph. (b) Block diagram.

TABLE I  
BASIC SPECIFICATIONS OF CLMR

Car-Like Mobile Robot	Length	387mm
	Width	295mm
	Height	150mm
Front-Wheel (Steering Wheel)	Weight	6.458 kg
	Diameter	127mm
	Thickness	40mm
	Wheelbase	255mm
Rear-Wheel (Drive Wheel)	Diameter	127mm
	Thickness	40mm
	Wheelbase	255mm
Height of Chassis	60mm	

are required. Before modeling the dc motors, a proportional feedback gain (i.e.,  $k_p^1 = 65$  volt/rad) for steering subsystem [see Fig. 11(a)] is employed to adjust its pole and DC gain. It is called “enhanced steering subsystem (ESS or ECLMR1).” Similarly, a forward gain  $k_p^2 = 100$  in Fig. 11(b) is applied

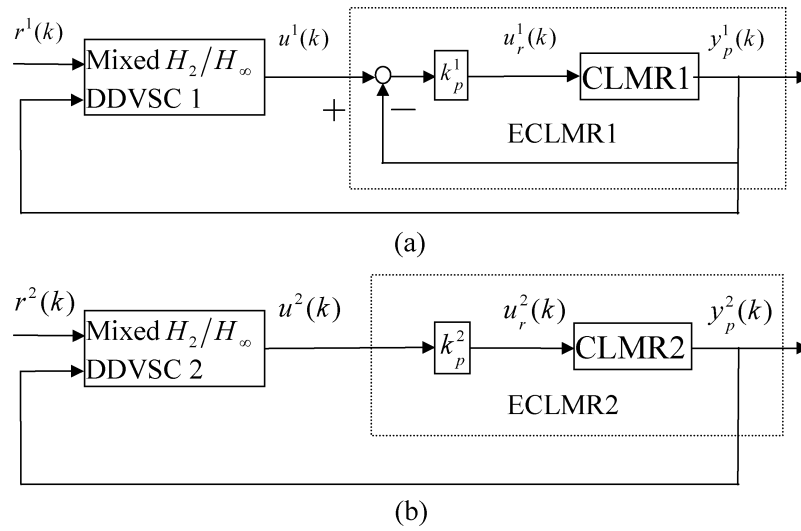


Fig. 11. Enhanced CLMR (ECLMR) by a proportional (feedback or forward) gain. (a) Steering angle. (b) Linear velocity.

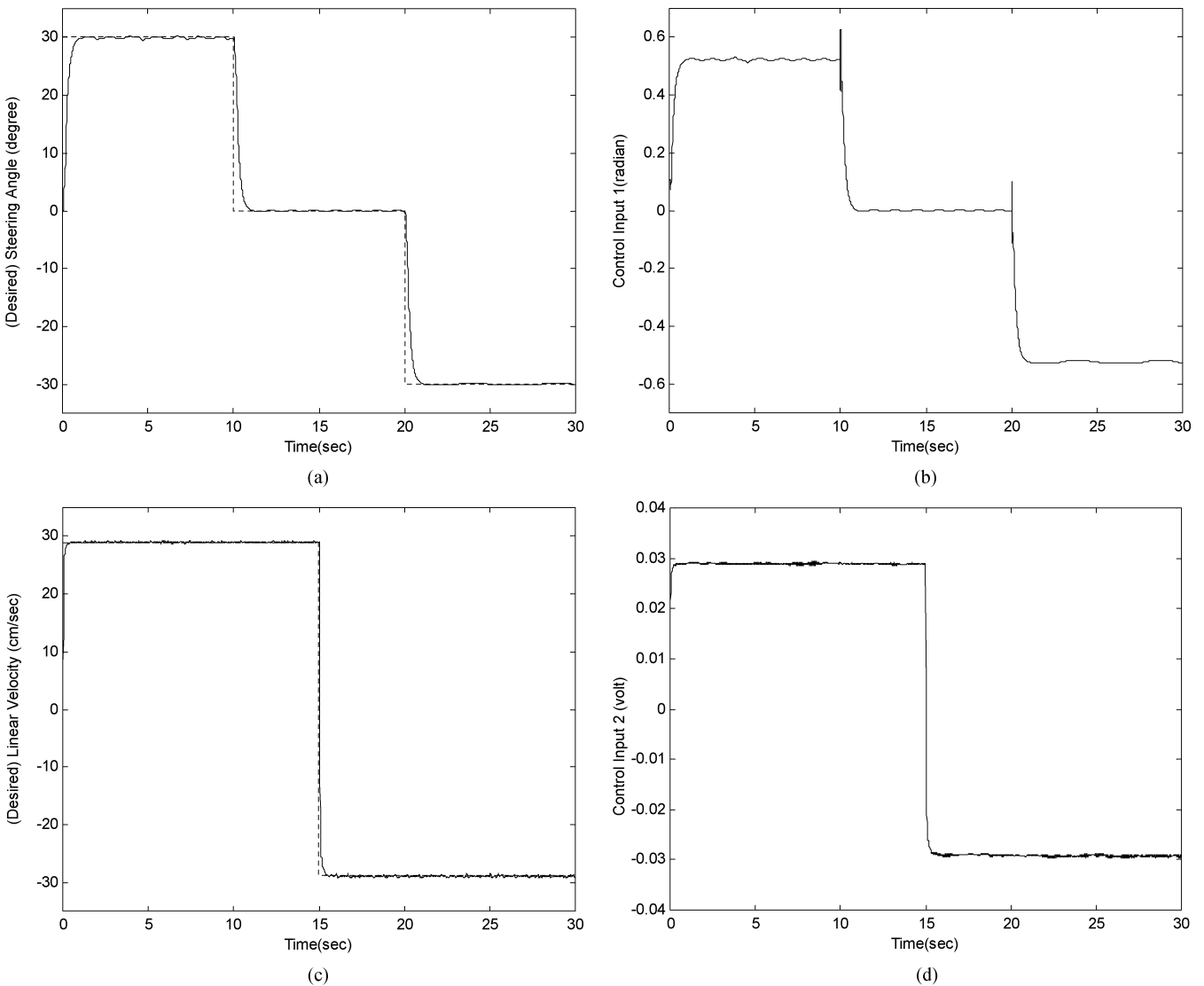


Fig. 12. Responses of the CLMR without load. (a)  $r^1(t)(\dots)$ ,  $y^1(t)(-)$ . (b)  $u^1(t)$ . (c)  $r^2(t)(\dots)$ ,  $y^2(t)(-)$ . (d)  $u^2(t)$ .

to obtain a unit DC gain of angular velocity subsystem. It is called “enhanced translating subsystem (ETS or ECLMR2).” After the model verification (e.g., sinusoidal response), the corresponding ECLMR is expressed as follows:

$$A^i(z^{-1}) = 1 + a_1^i z^{-1} + a_2^i z^{-2}$$

$$B^i(z^{-1}) = b_0^i + b_1^i z^{-1} \quad d^i = 1, i = 1, 2 \quad (51a)$$

$$a_1^1 = -1.259 \quad a_2^1 = 0.397$$

$$b_0^1 = 0.04834 \quad b_1^1 = 0.08702 \quad (51b)$$

$$a_1^2 = -0.895 \quad a_2^2 = 0.205$$

$$b_0^2 = 0.14357 \quad b_1^2 = 0.20125. \quad (51c)$$

### B. Response of CLMR Without Load

In the beginning, the CLMR is raised to evaluate the control performance of dc motors (i.e., steering angle and angular (or linear) velocity). Fig. 12 shows the response of two dc motors using the proposed control with parameters  $G_m^1(z^{-1})/F_m^1(z^{-1}) = (0.15 + 0.27z^{-1})/(1 - 0.7z^{-1} + 0.12z^{-2})$ ,  $G_m^2(z^{-1})/F_m^2(z^{-1}) = (0.05 + 0.07z^{-1})/(1 - 1.3z^{-1} + 0.42z^{-2})$ ,  $W_1^1(z^{-1}) = 0.003/(1 + 0.3z^{-1})$ ,  $W_1^2(z^{-1}) = 0.003/(1 + 0.85z^{-1})$ ,  $W_2^1(z^{-1}) = (1 - 0.6z^{-1})/(1 - 0.5z^{-1})$ ,  $W_2^2(z^{-1}) = (1 - 0.92z^{-1})/(1 - z^{-1})$ , and the same parameters of the switching control in Fig. 9. It indicates that the implementation of the proposed control is also satisfactory.

### C. Trajectory Tracking of CLMR

First, a trajectory of “S curve,” which is depicted as the dashed line of Fig. 13, is planned to test the performance of the proposed control system. One LED placed on the center of CLMR is detected by CCD in order to calculate the center position of the CLMR [see Fig. 10(a)]. Then the corresponding experimental result of the trajectory tracking for the CLMR is presented in Fig. 13, which has the maximum absolute tracking error 5 cm and again verifies the usefulness of our control method.

## VI. CONCLUSION

In this paper, a mixed  $H_2/H_\infty$  optimization for decentralized discrete variable structure control is established. The optimal  $J_1$  with a suitable weighted function ensures that the system in the presence of disturbance can obtain smaller energy consumption with bounded tracking error. The optimal  $J_2$  guarantees that the output disturbance caused by the interactions among subsystems, modeling error, and external load is attenuated. The proposed mixed  $H_2/H_\infty$  optimization does not need to calculate the Diophantine equation. It possesses the computational benefits especially for low-order system.

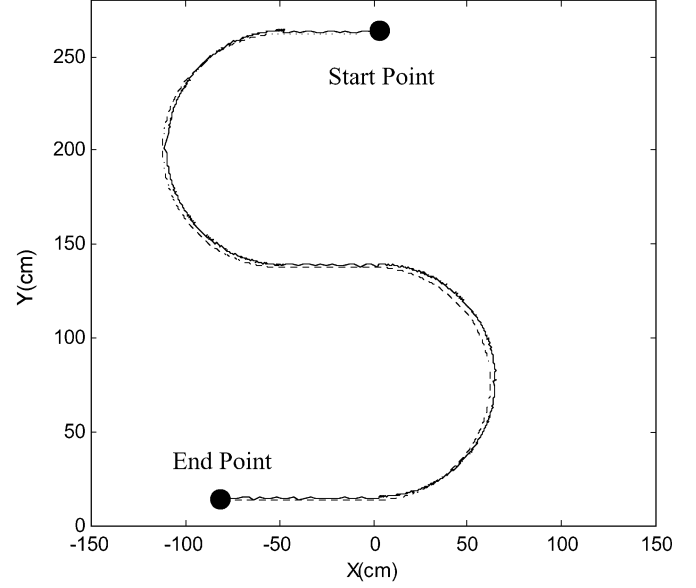


Fig. 13. Tracking response (—) of a CLMR for planning trajectory (---).

To further enhance the performance, a switching control in every subsystem is designed such that the robust performance and stability are improved. A suitable first weighted function can attenuate the response of the control input in the desired frequency range. Moreover, an appropriate second weighted function for rejecting the related output disturbance is more important than the role of a switching control. However, the switching control does not need the information of the output disturbance and can further enhance system performance. In addition, the off-line system identification and the controller design only for each subsystem are required. The stability of the closed-loop system is verified by Laypunov stability criterion. Finally, the simulations and experiments for the CLMR confirm the usefulness of the proposed control.

## APPENDIX

### Appendix A (The Proof of Lemma 1)

Substituting (16) into (15) gives

$$J_1 = \left\| \frac{G_m^i(z^{-1})G_r^i(z^{-1})}{F_m^i(z^{-1})F_r^i(z^{-1})} - \frac{T^i(z^{-1})C^i(z^{-1})G_r^i(z^{-1})}{W_{1d}^i(z^{-1})A_c^i(z^{-1})F_r^i(z^{-1})} \right\|_2. \quad (A1)$$

Substituting the factorization  $C^i(z^{-1})G_r^i(z^{-1}) = C_-^i(z^{-1})C_+^i(z^{-1})G_{r-}^i(z^{-1})G_{r+}^i(z^{-1})$  into the (A1) yields (A2), shown at the bottom of the page. Because  $(C_-^i(z^{-1})G_{r-}^i(z^{-1})) / (\bar{C}_-^i(z^{-1})\bar{G}_{r-}^i(z^{-1}))$  is an inner function,

$$J_1 = \left\| \frac{C_-^i(z^{-1})G_{r-}^i(z^{-1})}{\bar{C}_-^i(z^{-1})\bar{G}_{r-}^i(z^{-1})} \left[ \frac{\bar{C}_-^i(z^{-1})\bar{G}_{r-}^i(z^{-1})G_m^i(z^{-1})G_{r+}^i(z^{-1})}{C_-^i(z^{-1})F_m^i(z^{-1})F_r^i(z^{-1})} - \frac{\bar{C}_-^i(z^{-1})\bar{G}_{r-}^i(z^{-1})T^i(z^{-1})C_+^i(z^{-1})G_{r+}^i(z^{-1})}{W_{1d}^i(z^{-1})A_c^i(z^{-1})F_r^i(z^{-1})} \right] \right\|_2. \quad (A2)$$

based on the norm-preserving property of the inner function (A2) is simplified as

$$J_1 = \left\| \frac{\overline{C}_-(z^{-1})\overline{G}_{r-}(z^{-1})G_m^i(z^{-1})G_{r+}^i(z^{-1})}{C_-^i(z^{-1})F_m^i(z^{-1})F_r^i(z^{-1})} - \frac{\overline{C}_-(z^{-1})\overline{G}_{r-}(z^{-1})T^i(z^{-1})C_+^i(z^{-1})G_{r+}^i(z^{-1})}{W_{1d}^i(z^{-1})A_c^i(z^{-1})F_r^i(z^{-1})} \right\|_2. \quad (\text{A3})$$

Taking the decomposition of the first term in (A3) yields

$$\begin{aligned} \frac{\overline{C}_-(z^{-1})\overline{G}_{r-}(z^{-1})G_m^i(z^{-1})G_{r+}^i(z^{-1})}{C_-^i(z^{-1})F_m^i(z^{-1})F_r^i(z^{-1})} \\ = \frac{F_c^i(z^{-1})}{C_-^i(z^{-1})} + \frac{F_o^i(z^{-1})}{F_m^i(z^{-1})F_r^i(z^{-1})} \end{aligned} \quad (\text{A4})$$

for some polynomials  $F_c^i(z^{-1})$  and  $F_o^i(z^{-1})$ . Multiplying both sides of (A4) by  $C_-^i(z^{-1})F_m^i(z^{-1})F_r^i(z^{-1})$  gives

$$\overline{C}_-(z^{-1})\overline{G}_{r-}(z^{-1})G_m^i(z^{-1})G_{r+}^i(z^{-1}) = F_c^i(z^{-1})F_m^i(z^{-1})F_r^i(z^{-1}) + F_o^i(z^{-1})C_-^i(z^{-1}). \quad (\text{A5})$$

Because  $F_m^i(z^{-1})F_r^i(z^{-1})$  and  $C_-^i(z^{-1})$  are coprime, there exist unique polynomials  $F_c^i(z^{-1})$  and  $F_o^i(z^{-1})$ , where  $n_{f_c}^i = n_{c_-}^i - 1$  and  $n_{f_o}^i = n_{f_m}^i + n_{f_r}^i - 1$ . Or (A5) is rewritten as

$$F_o^i(z_j^i)C_-^i(z_j^i) - \overline{C}_-(z_j^i)\overline{G}_{r-}(z_j^i)G_m^i(z_j^i)G_{r+}^i(z_j^i) = 0 \quad (\text{A6})$$

where  $z_j^i$  for  $j = 1, 2, \dots, n_{f_o}^i$  are distinct zeros of  $F_m^i(z^{-1})F_r^i(z^{-1})$ . Finally,  $F_c^i(z^{-1})$  is readily determined from (A5) after obtaining the polynomial  $F_o^i(z^{-1})$  from (A6). Coupling (A4) and (A5) gives

$$J_1^2 = \left\| \frac{F_c^i(z^{-1})}{C_-^i(z^{-1})} + \frac{F_o^i(z^{-1})}{F_m^i(z^{-1})F_r^i(z^{-1})} - \frac{\overline{C}_-(z^{-1})\overline{G}_{r-}(z^{-1})T^i(z^{-1})C_+^i(z^{-1})G_{r+}^i(z^{-1})}{W_{1d}^i(z^{-1})A_c^i(z^{-1})F_r^i(z^{-1})} \right\|_2^2. \quad (\text{A7})$$

By orthogonal, it follows that

$$\begin{aligned} J_1^2 &= \left\| \frac{F_c^i(z^{-1})}{C_-^i(z^{-1})} \right\|_2^2 + \left\| \frac{F_o^i(z^{-1})}{F_m^i(z^{-1})F_r^i(z^{-1})} - \frac{\overline{C}_-(z^{-1})\overline{G}_{r-}(z^{-1})T^i(z^{-1})C_+^i(z^{-1})G_{r+}^i(z^{-1})}{W_{1d}^i(z^{-1})A_c^i(z^{-1})F_r^i(z^{-1})} \right\|_2^2 \\ &\geq \left\| \frac{F_c^i(z^{-1})}{C_-^i(z^{-1})} \right\|_2^2. \end{aligned} \quad (\text{A8})$$

Therefore, the optimal solution for the cost function (11) is described in (17) and (18), and the corresponding optimal value is given in (19). Q.E.D.

## Appendix B (The Proof of Theorem 1)

A Lyapunov candidate for the interconnected system is defined as follows:

$$V(k) = \sum_{i=1}^2 \frac{e_o^i(k)^2}{2} > 0, \quad \text{as } e_o^i(k) \neq 0. \quad (\text{B1})$$

The Lyapunov function defined in (B1) represents the total energy of the two subsystems in the interconnected system. Then the change of rate of (B1) is described as follows:

$$\Delta V(k) = \sum_{i=1}^2 \left\{ e_o^i(k)\Delta e_o^i(k) + \frac{\Delta e_o^i(k)^2}{2} \right\} \quad (\text{B2})$$

where  $\Delta e_o^i(k)$  is described in (37). The situation  $|e_o^i(k)| > \chi^i(k)$  is first considered. For ensuring the asymptotical convergence of the operating point to a convex subset, it is assumed that the inequality  $\Delta V(k) \leq -\varepsilon V(k)$  exists, where  $\varepsilon = \min_{1 \leq i \leq 2} (\varepsilon^i)$  and  $0 < \varepsilon^i < (1 - \lambda^i)^2 / (1 + \lambda^i)^2 < 1$ . Then the following (B3) and (B4) are achieved by (36)–(39), (B1), and (B2).

$$\begin{aligned} \Delta \overline{V}(k) &= \Delta V(k) + \varepsilon V(k) \\ &\leq \sum_{i=1}^2 e_o^i(k) \left\{ \Lambda^i(k) + [1 - \tau^i(z^{-1}, k)] v_{sw}^i(k) \right\} \\ &\quad + \sum_{i=1}^2 \frac{\left\{ \Lambda^i(k) + [1 - \tau^i(z^{-1}, k)] v_{sw}^i(k) \right\}^2}{2} \\ &\quad + \sum_{i=1}^n \frac{\varepsilon^i e_o^i(k)^2}{2} \\ &\leq \sum_{i=1}^2 \left\{ |e_o^i(k)| g_\lambda^i(k) - \frac{\xi^i(k) g_\lambda^i(k) |e_o^i(k)|}{1 + \lambda^i} \right. \\ &\quad \left. + \frac{g_\lambda^i(k)^2}{2} + \frac{\xi^i(k) g_\lambda^i(k)^2}{1 - \lambda^i} \right. \\ &\quad \left. + \frac{[\xi^i(k) g_\lambda^i(k)]^2}{2(1 - \lambda^i)^2} + \frac{\varepsilon^i e_o^i(k)^2}{2} \right\} \\ &= \sum_{i=1}^2 \left\{ \frac{g_\lambda^i(k)^2 g^i(\xi^i)}{[2(1 - \lambda^i)^2]} \right\} \end{aligned} \quad (\text{B3})$$

where

$$g^i(\xi^i) = \xi^i(k)^2 - 2g_1^i(k)\xi^i(k) + g_2^i(k). \quad (\text{B4})$$

If  $g^i(\xi^i) \leq 0$ , for  $i = 1, 2$  then  $\Delta \overline{V}(k) \leq 0$  (or  $\Delta V(k) \leq -\varepsilon V(k)$ ). Because

$$|e_o^i(k)| > \frac{4(1 + \lambda^i)g_\lambda^i(k)}{[(1 - \lambda^i)^2 - \varepsilon^i(1 + \lambda^i)^2]} \quad (\text{B5})$$

both  $g_1^i(k) > 0$  and  $g_1^i(k)^2 - g_2^i(k) > 0$  for  $i = 1, 2$  are achieved. Substituting (40) into (B5) yields

$$|e_o^i(k)| > \frac{4(1 + \lambda^i) \left( \sum_{j=1, j \neq i}^2 \lambda_{1j}^i |e_o^j(k)| + \lambda_2^i \right)}{[(1 - \lambda^i)^2 - \varepsilon^i(1 + \lambda^i)^2 - 4(1 + \lambda^i)\lambda_0^i]}. \quad (\text{B6})$$

From (B5) and (B6), the result (43) is achieved. In summary, the switching gain chosen from (44)–(47) makes  $\Delta V(k) \leq -\varepsilon V(k)$ . Then  $\{e_o^i(k), u^i(k)\}$ ,  $i = 1, 2$  are bounded and the performance (48) is accomplished.

Similarly, the case  $|e_o^i(k)| \leq \chi^i(k)$  is accomplished. Q.E.D.

#### ACKNOWLEDGMENT

The authors thank the valuable comments and suggestions from the reviewers.

#### REFERENCES

- [1] L. T. Grujic and D. D. Siljak, "Asymptotic stability and instability of large scale systems," *IEEE Trans. Automat. Contr.*, vol. AC-18, no. 6, pp. 636–645, Dec. 1973.
- [2] D. D. Sijak, *Large-Scale Dynamic Systems: Stability and Structure*. Amsterdam, The Netherlands: North-Holland, 1978.
- [3] W. S. Chan and C. A. Desoer, "Eigenvalue assignment and stabilization of interconnected systems using local feedbacks," *IEEE Trans. Automat. Contr.*, vol. AC-24, no. 2, pp. 312–317, Apr. 1979.
- [4] Y. H. Chen, "Decentralized robust control system design for large-scale uncertain systems," *Int. J. Contr.*, vol. 111, pp. 1195–1205, 1988.
- [5] C. S. Tseng and B. S. Chen, " $H_\infty$  decentralized fuzzy model reference tracking control design for nonlinear interconnected systems," *IEEE Trans. Fuzzy Syst.*, vol. 9, no. 6, pp. 795–809, Dec. 2001.
- [6] J. H. Lee and H. Hashimoto, "Controlling mobile robots in distributed intelligent sensor network," *IEEE Trans. Ind. Electron.*, vol. 50, no. 5, pp. 890–902, Oct. 2003.
- [7] X. Chen, K. Watanabe, K. Kiguchi, and K. Izumi, "An ART-based fuzzy controller for the adaptive navigation of a quadruped robot," *IEEE/ASME Trans. Mechatron.*, vol. 7, no. Sep., pp. 318–328, 2002.
- [8] J. C. Doyle, K. Glover, P. P. Khargonekar, and B. Francis, "State-space solutions to standard  $H_2$  and  $H_\infty$  problems," *IEEE Trans. Automat. Contr.*, vol. 34, no. 8, pp. 831–847, 1989.
- [9] B. S. Chen and W. Zhang, "Stochastic  $H_2/H_\infty$  control with state-dependent noise," *IEEE Trans. Automat. Contr.*, vol. 49, no. 1, pp. 45–57, Jan. 2004.
- [10] J. Chen, S. Hara, and G. Chen, "Best tracking and regulation performance under control energy constraint," *IEEE Trans. Automat. Contr.*, vol. 48, no. 8, pp. 1320–1336, Aug. 2003.
- [11] C. L. Hwang and C. Jan, "Optimal and reinforced robustness designs of fuzzy variable structure tracking control for a piezoelectric actuator system," *IEEE Trans. Fuzzy Syst.*, vol. 11, no. 4, pp. 507–517, Aug. 2003.
- [12] Y. Hung, W. Gao, and J. C. Hung, "Variable structure control: a survey," *IEEE Trans. Indust. Electron.*, vol. 40, no. 1, pp. 2–22, Jan. 1993.
- [13] K. D. Young, V. I. Utkin, and Ü. Özgüner, "A control engineer's guide to sliding mode control," *IEEE Trans. Contr. Syst. Technol.*, vol. 7, no. 3, pp. 328–342, May 1999.
- [14] K. Furuta and Y. Pan, "Variable structure control with sliding sector," *Automatica*, vol. 36, no. 3, pp. 211–228, 2000.
- [15] C. L. Hwang, "Robust discrete variable structure control with finite-time approach to switching surface," *Int. J. Automatica*, vol. 38, no. 1, pp. 167–175, 2002.
- [16] H. K. Khalil, *Nonlinear Systems*, 2nd ed. Upper Saddle River, NJ: Prentice-Hall, 1996.
- [17] M. Vidyasagar, *Controller System Synthesis—A Factorization Approach*. Cambridge, MA: MIT Press, 1995.
- [18] C. L. Hwang and B. S. Chen, "Adaptive control of optimal model matching in  $H^\infty$ -norm space," *Proc. Inst. Elect. Eng., Contr. Theory, Applicat.*, vol. 135, no. 4, pp. 295–301, 1988.



**Chih-Lyang Hwang** (A'04) received the B.E. degree in aeronautical engineering from Tamkang University, Taipei, Taiwan, R.O.C., in 1981, and the M.E. and Ph.D. degrees in mechanical engineering from Tatung Institute of Technology, Taipei, in 1986 and 1990, respectively.

Since 1990, he has been with the Department of Mechanical Engineering, Tatung Institute of Technology, where he is engaged in teaching and research in the area of servo control and control of manufacturing systems. Since 1996, he has been a

Professor of mechanical engineering with the Tatung Institute of Technology. In 1998–1999, he was a Research Scholar of the George W. Woodruff School of Mechanical Engineering, Georgia Institute of Technology. At present, he is a committee member in Automation Technology of National Science Council of Taiwan. He is the author or coauthor of about 80 journal and conference papers in the related field. His current research interests include fuzzy (neural network) modeling and control, variable structure control, mechatronics, robotics, visual tracking system, and network-based control.

Dr. Hwang has received a number of awards, including the Excellent Research Paper Award from the National Science Council of Taiwan and Hsieh-Chih Industry Renaissance Association of Tatung Company. He was a member of the technical committee of IEEE IECON02.



**Song-Yu Han** was born in Taiwan, R.O.C., in 1981. He received the B.E. degree and the M.E. degree in mechanical engineering from Tatung University, Taipei, in 2003 and 2004, respectively, where he is currently working toward the Ph.D. degree in mechanical engineering.

His current research interests include fuzzy control system, mobile robot, robust control, and mechatronics.